# An Analytical Method to Find the Optimal Parameters for Gas Detectors based on Correlation Spectroscopy using a Fabry-Perot Interferometer.

**Everardo Vargas-Rodríguez, and Harvey N. Rutt**

*Optoelectronics Research Centre, University of Southampton,*

*Bldg. B47, Highfield Campus, SO17 1BJ, Southampton, United Kingdom..*

*fax: +44 (0) 2380593149, email: evr@orc.soton.ac.uk*

**Abstract**

Several designs of infrared sensors use a Fabry-Perot Interferometer (FPI) to modulate the incident light. In this work we analyse the particular case where the FPI fringes are matched with very well defined ro-vibrational absorption lines of a target molecule such as $CO_2$, CO, $N_2O$, or $CH_4$. In this kind of sensor modulation is induced by scanning the FPI cavity length over one half of the reference wavelength. Here we present an analytical method based on the Fourier transform which simplifies the procedure to determine the sensor response. Furthermore, this method provides a simple solution to finding the optimal FPI cavity length and mirror reflectivity. It is shown that FPI mirrors with surprisingly low reflectivity (<50%) are generally the optimum choice for target gases at atmospheric pressure. Finally experimental measurements and simulation results are presented.

***OCIS Codes:*** 120.2230, 300.6340, 130.6010, 220.4830, 070.2590.

# 1 Introduction

Detectors based on correlation spectroscopy that use a Fabry-Perot Interferometer (FPI) as a modulator are appropriate for detection of molecules with very well defined ro-vibrational absorption lines with pressure-broadened Lorentzian line shapes.[1-6] These lines are characteristic of most diatomic and linear molecules, i.e. $CO_2$, CO, $N_2O$, and some specific absorptions bands of symmetric top and spherical top molecules, i.e. $NH_3$, $CH_4$ at one atmosphere pressure. In these sensors the modulation is induced, firstly, by matching the FPI's fringes with the ro-vibrational absorption lines of the target molecule (Fig. 1a), and then by scanning the cavity length over one half of the reference wavelength $(\lambda_0/2)$. This scan produces a shift of the FPI's fringes along the wavenumber axis (Fig. 1b) producing a transmission change through the system, and therefore producing an intensity modulation. The integrated transmission through the system at normal incidence is given by

$$I_D(R,n,d,\delta) = \int_0^\infty I_{FP}(\nu,R,n,d,\delta)\, T(\nu)\, Fil(\nu)\, S(\nu)\mathrm{d}\nu, \qquad (1)$$

where $\nu$ is the frequency expressed in wavenumbers (1/cm), $I_{FP}(\nu,R,n,d,\delta)$ describes the FPI fringe pattern, $d$ is the FPI cavity length, $R$ is the reflectivity, *n* is the refractive index of the medium between the FPI's mirrors, and $\delta$ represents the instantaneous value of the cavity length scan $(0 \le \delta \le \lambda_0/2)$. The band pass filter transmission is given by $Fil(\nu)$, the transmission through the gas pathlength is defined by $T(\nu)$, and the source spectral profile is defined by $S(\nu)$. The amplitude of the sensor signal $I_D(R,n,d,\delta)$ is directly related to the gas concentration. The amplitude of this signal, amplitude modulation $(AM)$ of the infrared signal, is the

difference between the maximum and the minimum values of $I_D(R, n, d, \delta)$ which can be expressed as

$$AM = I_D(R, n, d, \delta)_{\max} - I_D(R, n, d, \delta)_{\min}. \quad (2)$$

It is clear that the sensor response $I_D(R, n, d, \delta)$ depends on several parameters which increase the complexity of the sensor design. Optimum sensor design requires us to have the maximum possible amplitude modulation when the target gas is present, ie when $T(\nu) \neq 1$. But it also requires the minimum amplitude modulation when the target gas concentration is zero, that is when $T(\nu) = 1$, which we refer to as background modulation. High levels of background modulation are extremely undesirable, as any instability in this value limits the minimum detectable gas concentration. The simplest way to find the optimum values for $R$, $nd$, and $\delta$ is by direct numerical evaluation of equation (1). Here, the parameter values are changed simultaneously looking for a combination that provides the best compromise between the minimum background modulation and the maximum amplitude modulation. However, whilst this method is very simple to implement it is time consuming since it takes a long time to compute all the possible parameter values combinations ($0 \leq R \leq 1$, $0 \leq nd \leq \infty$, and $0 \leq \delta \leq \lambda_0/2$). Furthermore the same procedure must be repeated for different filter responses $Fil(\nu)$ in order to determine which band pass filter is the best for the application. We have found that some filter band pass shapes can seriously affect the background modulation as we previously reported in detail.[7] In that work we reported that filters with very abrupt transitions from the stop to pass band are in fact undesirable, and that simple low cost band pass filters are often the best choice. In this work we present a new approach based on the Fourier transform which helps to evaluate much more rapidly the sensor response $I_D(R, n, d, \delta)$ in

comparison with the direct numerical evaluation of equation (1). Moreover it is shown that using this method the optimum optical thickness of the FPI $(nd)$ can be easily determined. This method also simplifies the procedure to find the optimum $R$ value. Furthermore, it is shown that if the modulated sensor signal $I_D(R, n, d, \delta)$ will be recovered by a Phase Sensitive Detector (PSD, also known as a lock-in amplifier) the optimum $R$ value is 0.41 regardless of the target gas.

## 2 System Response described as a convolution

As was stated above, to induce modulation the FPI's fringes are shifted along the wavenumber axis by scanning the FPI cavity length. A cavity length scan within the range $(0 \leq \delta \leq \lambda_0/2)$ produces a shift in the FPI fringes equivalent to one Free Spectral Range (FSR) which is the spectral separation between two consecutive FPI fringes.[8] As the FPI's fringe position is shifted along the wavenumber axis $(\Delta\nu)$ due to the cavity length scan $(\delta)$ therefore it is convenient to make a variable change in Eq. (1) as follows:

$$I_D(R, n, d, \Delta\nu) = \int_0^\infty I_{FP}(\nu, R, n, d, \Delta\nu)\, T(\nu)\, Fil(\nu)\, S(\nu) \mathrm{d}\nu. \tag{3}$$

As the filter transmission $Fil(\nu)$, the transmission through the gas pathlength $T(\nu)$, and the source profile $S(\nu)$ do not change while the cavity length is varied it is possible to express the product of these functions as

$$G(\nu) = S(\nu)\, Fil(\nu)\, T(\nu). \tag{4}$$

Hence Eq. (2) can be expressed as

$$I_D\left(R,n,d,\Delta\nu\right)=\int_0^\infty I_{FP}\left(\nu,R,n,d,\Delta\nu\right)G\left(\nu\right)\mathrm{d}\nu. \tag{5}$$

Now, considering that the shape and the symmetry of the FPI's fringes do not change when they are shifted by one Free Spectral Range (FSR) equation Eq. (4) can be rewritten as

$$I_D\left(R,n,d,\Delta\nu\right)=\int_0^\infty I_{FP}\left(\Delta\nu-\nu,R,n,d\right)G\left(\nu\right)\mathrm{d}\nu, \tag{6}$$

Therefore the system response expressed by equation (1) can be reduced and expressed as equation (6) which has the form of

$$h\left(t\right)=\int_{-\infty}^\infty f\left(\tau-t\right)k\left(t\right)\mathrm{d}\tau \tag{7}$$

which is the definition of the convolution function. Therefore, the system can be solved in a very simple way by using the Fourier transform properties. It is important to recall that the Fourier transform of a convolution $(*)$ is given by

$$\mathbf{FT}\left\{f\left(t\right)*k\left(t\right)\right\}=H\left(\omega\right)=F\left(\omega\right)K\left(\omega\right); \tag{8}$$

Therefore, the Fourier transform of Eq. (6) can be expressed as

$$\mathbf{FT}\left\{I_D\left(R,n,d,\Delta\nu\right)\right\}=I_D\left(R,n,d,\xi\right)=I_{FP}\left(\xi,R,n,d\right)G\left(\xi\right); \tag{9}$$

Hence, to solve the convolution given by Eq. (6) it is just necessary to evaluate the Fourier transform of two functions as given by Eq. (9). Finally to obtain the modulated signal produced by the system $I_D\left(R,n,d,\delta\right)$ we need to apply the inverse Fourier transform to Eq. (9). In the next section we analyze the characteristics of the

Fourier transform of the functions involved in Eq. (9) and using these characteristics we develop our approach to determine the optimum parameter values.

# 3 Fourier transforms characterization of the system functions.

In this section will be show that the optimal parameters *nd*, and *R* can be obtained using the characteristics of the Fourier transforms of the system functions $I_{FP}(\xi, R, n, d)$ and $G(\xi)$. Consequently, the detector will be optimized for the filter shape, for the source and for the ro-vibrational absorption lines of the target gas.

## *3.1 Fourier transform of the FPI's fringe transmission pattern*

For simplicity we will start by analysing the Fourier transform of the FPI's transmission fringe pattern described by the Airy formula.[9] Here, for clarity it is convenient to use the Fourier series expansion of the Airy function[10]

$$I_{FP}(\nu, R, n, d, \theta) = \frac{(1-R)}{(1+R)}\left\{1 + 2\sum_{m}^{\infty} R^m \cos\left(m4\pi nd\nu\cos(\theta)\right)\right\}; \qquad (10)$$

where $\theta$ is the angle of incidence and therefore for a collimated beam at normal incidence $\cos\theta = 1$. Therefore, from Eq. (10) it is possible to observe that the Airy function is given by a sum of a DC component and cosine functions of 'frequencies' $\xi = m2nd$, at normal incidence. These 'frequencies' are due to the period of the fringes, given by the $\mathrm{FSR} = 1/(2nd)$. Thus, the first harmonic (fundamental) of the Airy Function has a 'frequency' of $2nd$, the second harmonic has a 'frequency' of

$4nd$, the third harmonic of $6nd$, and so on. Moreover, the amplitudes of these cosine functions are given by

$$A_m = \frac{(1-R)}{(1+R)} 2R^m \qquad m = 1, 2, ..\infty \tag{11}$$

Therefore the Fourier transform of the Airy function consists in a set of impulses centred at 'frequencies' $\xi = \pm m2nd$ and magnitude $A_m/2$, which can be expressed as

$$I_{FP}(\xi, R, n, d) = \begin{cases} \frac{A_m}{2} & |\xi| = m2nd \\ 0 & |\xi| \neq m2nd \end{cases} \tag{12}$$

For instance consider a FPI to be used for detecting $CO_2$ at 4.3 μm with a mirror reflectivity $R = 0.3$ and a cavity length $d = 0.28$ cm, whose transmittance is shown in Figure 2a, and its Fourier transform is shown in Figure 2b. Here it is possible to observe in the Fourier transform spectrum that the first impulse occurs at $\xi = 2nd = 0.56$ cm, with $n = 1$. From Eqs. (11 and 12) we see that the position of the impulses in Fourier due to the FPI fringes depends directly on the optical thickness value $(nd)$ and their magnitude depends directly on the reflectivity $(R)$.

### *3.2 Fourier Transform characteristics of the $G(\nu)$ function, and the optimum* nd *parameter value.*

The function $G(\nu)$ represents the product of the source profile the filter performance and the transmission through the gas path length as stated in Eq. (4). In figure 3a an example of a $G(\nu)$ profile it is shown; in this example we are considering a measured filter performance in combination with a simulated $CO_2$ absorption spectrum at 4.3 μm with a gas path length of 2 cm and a $CO_2$ concentration of 300

ppm. The Fourier transform of the $G(\nu)$ spectrum is shown in figure 3b where some side-lobes at certain frequencies are clearly defined. The side-lobe positions in the Fourier spectrum give information related to the separation of the ro-vibrational absorption lines. The peak value of the first side-lobe represents the effective average line spacing in the band, whilst the width of the peak indicates the degree of variation in line spacing, caused primarily by differing upper and lower state ro-vibrational constants. In figure 3b it is clear how the magnitude of the side-lobes increases with the gas concentration whilst the magnitude for the other frequencies remains very close to zero. Therefore, as the amplitude modulation of the system is described by a convolution, whose Fourier transform is given by Eq. (9), the modulated signal produced by the system will be maximum if we make that the first impulse frequency of $I_{FP}(\xi, R, n, d)$ coincide with the frequencies where the first side-lobe peak of $|G(\xi)|$ occurs. Thus once $|G(\xi)|$ has been calculated we simply look for the frequency $(\xi_{\max})$ where the largest side-lobe peak of $|G(\xi)|$ occurs (Fig. 3b). After $\xi_{\max}$ is found the optimum value for the optical thickness of the FPI can be derived as $nd = \xi_{\max}/2$.

### *3.3 Evaluation of the amplitude modulation (*AM*).*

The amplitude of the modulated sensor response $(AM)$, can be easily evaluated using our convolution method approach which consists of the following five steps

1. Evaluate the two Fourier transforms $\mathbf{FT}\{I_{FP}(\nu, R, n, d)\}$ and $\mathbf{FT}\{G(\nu)\}$.
2. Multiply these Fourier transforms functions to obtain $I_D(R, n, d, \xi) = I_{FP}(R, n, d, \xi)G(\xi)$.

3. To get the system response as a function of the wavenumber shift apply the inverse Fourier transform to the previous product, $I_D(R,n,d,\Delta\nu) = \mathbf{IFT}\{I_{FP}(R,n,d,\xi)G(\xi)\}$.
4. From $I_D(R,n,d,\Delta\nu)$ extract the segment corresponding to $0 \le \Delta\nu \le \mathrm{FSR}$ which is equivalent to a cavity length scan $0 \le \delta \le 1/(2n\lambda_0)$. The system response is now in function of the cavity length scan $I_D(R,n,d,\delta)$.
5. Finally to get *AM* evaluate the difference between the maximum and the minimum of the system response as $AM = I_D(R,n,d,\delta)_{\max} - I_D(R,n,d,\delta)_{\min}$.

The main advantage of this convolution method is that it can evaluate the sensor response much faster than the numerical evaluation of Eq. (1). Furthermore, using the Fourier transform characterization of the functions gives a better insight into the system design.

For instance, let us evaluate the amplitude modulation as a function of the concentration for a $CO_2$ gas sensor using the following parameters:

- Ro-vibrational lines of $CO_2$ in the 4.3 μm region.
- A fixed gas pathlength of $l = 10$ cm;
- a flat source profile $S(\nu)$;
- a band pass filter, which is described in figure 3a.
- The FPI has a fixed $R = 0.30$, and the optical thickness $nd = 0.28$ cm.
- The gas concentration is varied from 0 to 1000 ppm.

The amplitude modulation for this sensor obtained by both the convolution and the direct calculation methods are presented in figure 4. The results are practically the same however the convolution method is considerably faster than the direct numerical calculation of equation (1).

### 3.4 Evaluation of the optimum $R$ value

In order to determine the optimum value of the FPI mirrors reflectivity $(R)$ it is necessary to evaluate the system response $I_D(R, n, d, \delta)$ considering the possible values of the reflectivity $(0 \leq R \leq 1)$. This can be done easily using the convolution method since here we know the optimum value of the optical thickness $(nd)$, see section 3.2. Therefore evaluation of Eq. (9) for different values of $R$ implies that if the gas concentration does not change the function $G(\xi)$ remains constant and only $I_{FP}(\xi, R, n, d)$ needs to be evaluated for each $R$ value, greatly reducing the number of computational operations. In this way $I_D(R, n, d, \delta)$ is obtained by applying the inverse Fourier transform of Eq. (9) for each value *R*. A plot showing the amplitude modulation $(AM)$ values as a function of the reflectivity obtained using both methods, the convolution method and by direct numerical evaluation of Eq. (1), is presented in figure 5. The results obtained by both method are practically the same and it can be appreciated that for the case with $nd = 0.28$ the optimum $R$ value is around $R_{\mathrm{O}} = 0.45$ where the maximum amplitude modulation is obtained. Additionally from figure 5 it can be seen that FPI mirrors with reflectivity values within the range from $0.2$ to $0.7$ will produce $AM$ values very close to the optimum. This result relaxes the FPI requirements since it shows that a relatively low reflectivity is required to get the maximum amplitude modulation.

The surprisingly broad, low reflectivity occurs due to the compromise between the overall power reaching the detector and the depth of modulation. These factors are directly related to the amplitude of the different components of the FPI fringe pattern. The magnitude of the first 4 harmonics and the DC component of $I_{FP}(\xi, R, n, d)$ as a

function of the reflectivity are shown in figure 6. Hence if we select a low reflectivity $(R < 0.2)$ we will have a quasi-sinusoidal FPI fringe pattern of relatively low amplitude, causing a low depth modulation regardless of the high overall power reaching the detector (high DC component). In the other extreme by selecting a relatively high reflectivity $(R > 0.7)$ the overall power reaching the detector is considerably reduced. Furthermore, for high $R$ the higher components of the FPI fringe pattern are more significant, which means that the overall power is distributed between all the components. Hence the amplitude of the fundamental component of the FPI fringe will be low producing a low depth of modulation that in combination with low overall power causes a low $AM$ sensor response. Therefore the broad, flat maximum peaking of $AM$ at relatively low reflectivity values is due to the compromise between the depth of modulation and the overall power arriving at the detector.

If the system response $I_D\left(R, n, d, \delta\right)$ is recovered by a phase sensitive detector (PSD) just the first harmonic (fundamental) of the modulated signal produced by the detector is retrieved whilst the rest of the harmonics are rejected. The fundamental of $I_D\left(R, n, d, \delta\right)$ depends directly of the first impulse of $I_{FP}\left(\xi, R, n, d\right)$ (Fig. 6). Consequently, to get the maximum $AM$ for the fundamental we need to get the maximum magnitude possible for the first impulse of $I_{FP}\left(\xi, R, n, d\right)$. The magnitude of the first impulse of $I_{FP}\left(\xi, R, n, d\right)$ can be expressed as

$$\mid I_{FP}\left(2nd, R, n, d\right) \mid = \frac{(1-R)}{(1+R)} R. \tag{13}$$

By differentiation of Eq. (13) we find that the maximum of this function occurs when $R = 0.41$ (Fig. 6). Here with $R_O = 0.41$ the fundamental component of the FPI fringe pattern has its maximum amplitude (Fig. 6) which maximizes the amplitude of the fundamental component of the sensor response. Therefore when using a PSD to get the maximum amplitude modulation the optimum reflectivity is $R_O = 0.41$, independent of the other system parameters.

## 4 Experimental results

In order to prove our convolution method we constructed a FPI based gas sensor as shown in figure 7, and the results are presented in this section. The FPI fringe pattern considering a blackbody converging source can be evaluated using the following formula:

$$I_{FP}(\nu, R, n, d) = \frac{2}{\sin^2(\theta_{\max})} \int_0^{\theta_{\max}} I_{FP}(\nu, R, n, d, \theta) \sin\theta \cos\theta \mathrm{d}\theta. \qquad (14)$$

By selecting low $\theta_{\max}$ values the FPI fringes are only slightly affected by the converging beam and therefore the FPI fringe pattern is similar to the pattern produced by a parallel beam. Hence using a low $\theta_{\max}$ value will allow us to use directly the convolution method as the shape and the symmetry of the FPI fringes is not seriously affected.

### *4.1 $CH_4$ Gas Sensor Design*

In this experiment we used as FPI mirrors two $CaF_2$ substrates coated on one side with a ZnS thin layer of 470 nm, the substrates were wedged to reduce fringes generated within the substrate. The measured spectral reflectivity of the FPI mirrors is

shown in figure 8, measured using a FTIR Perkin Elmer Spectrum GX. These mirrors have a broad reflectivity $R \approx 0.30$ from 4.7 to 4.2 μm (for CO and $CO_2$) and $R \approx 0.28$ at 3 μm where a fundamental band of $CH_4$ occurs. Moreover in this experiment we use $CaF_2$ windows for the gas cell and a 10 cm focal length $CaF_2$ biconvex lens. The iris diaphragm is intended to control the maximum angle of incidence $\theta_{\max}$.

For this design the converging cone angle was fixed to $\theta_{\max} = 0.0416$ rad in order to minimize the effect on the FPI fringe pattern (Fig. 9), here just a small loss in the fringe contrast is observed. We used a band pass filter centred at 3.2 μm where the strongest fundamental band of $CH_4$ occurs. The filter performance is presented in Figure 10a when the $CH_4$ concentration is 0% as $G(\nu) = Fil(\nu)$. In this experiment we used a gas cell with path length $(l)$ of 1.4 cm, a thermal source IR-12 from Scitec Instruments operated at 1074K, and the LTI Q1 pyroelectric detector from DIAS Infrared Systems.

The first step in the sensor design consists in the evaluation of the function $G(\nu) = S(\nu)\,T(\nu)\,Fil(\nu)$. Here as the source is an almost flat blackbody source in the filter band pass region therefore $G(\nu) = T(\nu)\,Fil(\nu)$ (Fig. 10a). By applying the Fourier transform to this function the optimum optical thickness $nd$ can be obtained. The magnitude of this Fourier transform for different gas concentration is shown in figure 10b where it is seen that the maximum amplitude modulation occurs when $nd = \xi_{\max}/2 = 0.055$ cm. To prove this value we varied the cavity length $d$ in our experiment from $0.045$ to $0.065$ cm looking for the maximum $AM$ value. The simulated results and the experimental measurements are in agreement as shown in

figure 11, they also show that the optimal optical thickness $nd = \xi_{\max}/2 = 0.055$ obtained by the analysing function $|G(\xi)|$ is correct. Finally the simulation results and the experimental measurement of $AM$ as a function of the gas concentration are shown in are shown in Figure 12. The convolution method results were obtained by using the procedure presented in section 3.3 which produces practically the same results as the obtained with by direct evaluation of Eq. (1) but much more rapidly. The measurements are in very good agreement with our simulation results.

## 5 Conclusions

We have presented an analytical method which helps us to evaluate much faster the response of gas sensors which use a FPI as a modulator. This method also provides a simple solution to determine the optimum parameters $nd$ and $R$ of the FPI. It is shown that relatively low reflectivity values are a good choice for these sensors relaxing the design of the system since FPI mirrors with high $R$ are generally very expensive. Furthermore it is shown that if the sensor signal will be recovered with a Phase Sensitivity Detector the optimum mirror reflectivity is $R = 0.41$, independent of other system parameters.

## 6 Acknowledgments

E. Vargas-Rodríguez is grateful to the Mexican National Council for Science and Technology (CONACyT) for a student research grant.

# 7 References


1. J. J. Barrett, and S. A. Myers, "New Interferometric Method for Studying Periodic Spectra Using a Fabry-Perot Interferometer," J. Opt. Soc. Am. B **61**(9), 1246-1251 (1971).

2. W. Jin, G. Stewart, B. Culshaw, S. Murray, and D. Pinchbeck, "Absorption measurement of methane gas with a broadband light and interferometric signal processing," Optics Letters **18**(16), 1364-1366 (1993).

3. J. P. Dakin, C. A. Wade, D. Pinechbeck, and J. S. Wykes, "A novel fibre methane sensor," Proc. SPIE **734**, 254-260 (1987).

4. A. Mohebati, and T. A. King, "Remote detection of gases by diode laser spectroscopy," Journal of Modern Optics **35**(3), 319-324 (1988).

5. J. P. Dakin, "Review of Fibre Optic Gas Sensors," in *The Plessey Company PLC*, (1988).

6. W. Jin, G. Stewart, B. Culshaw, and S. Murray, "Source-noise limitation of fiber-optic methane sensors," Applied Optics **34**(13), 2345-2349 (1995).

7. E. Vargas-Rodriguez, and H. N. Rutt, "Method to minimize spurious background signals in gas detectors based on correlation spectroscopy using a Fabry-Perot bandpass filter shape optimization," Optical Engineering **44**(10), 103002 (2005).

8. E. Hecht, *Optics* (Addison Wesley, United States of America, 1998).

9. M. Born, and E. Wolf, *Principles of Optics* (Pergamon Press, Great Britain, 1965).

10. J. M. Vaughan, *The Fabry-Perot Interferometer History, Theory, practice and applications* (Adam Hilger, USA, 1989).

## Figure Captions

Figure 1 Fabry-Perot fringes and target molecule ro-vibrational absorption lines. a) FPI's fringes matched with the ro-vibrational lines; b) FPI's fringes shifted along the wavenumber axis. The ro-vibrational lines are shifted up for clarity.

Figure 2 FPI transmission fringes characteristics and its Fourier transform. a) Transmission fringe profile considering $R = 0.30$ and $nd = 0.28$ cm; b) Fourier transform of the FPI fringes.

Figure 3 a) Function $G(\nu)$ profile showing the filter performance and the ro-vibrational absorption lines of $CO_2$ and considering a flat source b) Fourier transform of $G(\nu)$, here the magnitude of the side-lobes centred at $\xi = 0.56$ cm clearly increase with the $CO_2$ concentration.

Figure 4 Amplitude Modulation for a $CO_2$ sensor evaluated using both the direct numerical evaluation of equation (1) and using the convolution method. Here $R = 0.30$ and $nd = 0.28$ cm.

Figure 5 Amplitude modulation as a function of the reflectivity with a constant optical thickness $nd = 0.28$ cm. Different $CO_2$ concentrations are shown.

Figure 6 Magnitude of the FPI fringes impulses as a function of the reflectivity.

Figure 7 Experimental Setup.

Figure 8 Measured FPI Mirror reflectivity.

Figure 9 FPI fringe patterns evaluated for a collimated beam ($\theta_{\max} = 0\text{rad}$) and for a converging beam with $\theta_{\max} = 0.0416$ rad.

Figure 10 a) Function $G(\nu)$ for the $CH_4$ sensor for different gas concentrations. b) Magnitude of the Fourier transform $|G(\xi)|$.

Figure 11 Simulated and Measured Amplitude Modulation values for the $CH_4$ sensor. Here we use $R = 0.30$ and $CH_4$ Concentration of 50%.

Figure 12 Simulated and Measured $AM$ values in function of the $CH_4$ Concentration.

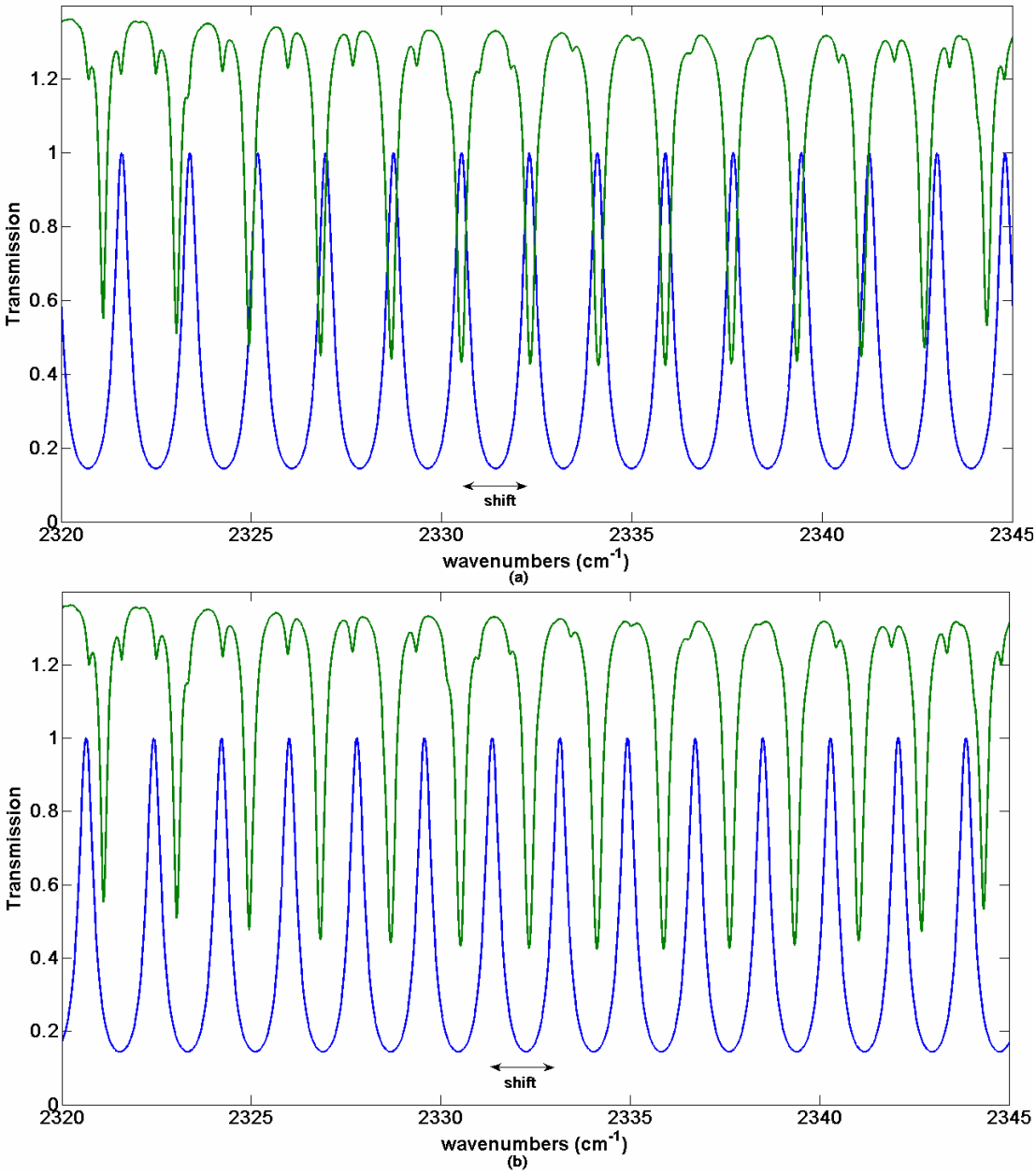


Figure 1- Fabry-Perot fringes and target molecule ro-vibrational absorption lines. a)FPI's fringes matched with the ro-vibrational lines; b) FPI's fringes shifted along the wavenumber axis. The ro-vibrational lines are shifted up for clarity.

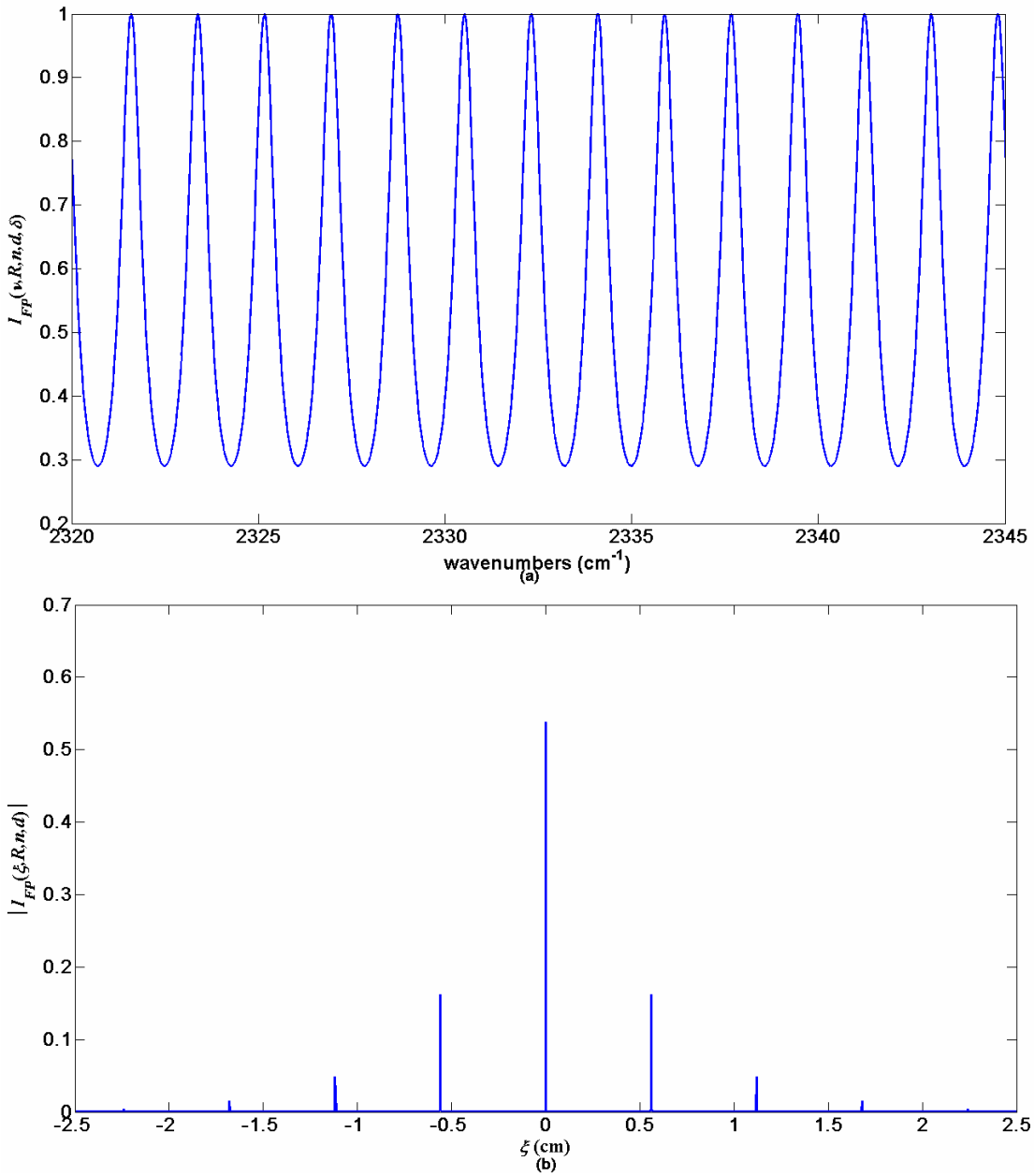


Figure 2- FPI transmission fringes characteristics and its Fourier transform. a) Transmission fringe profile considering $R = 0.30$ and $nd = 0.28$ cm; b) Fourier transform of the FPI fringes.

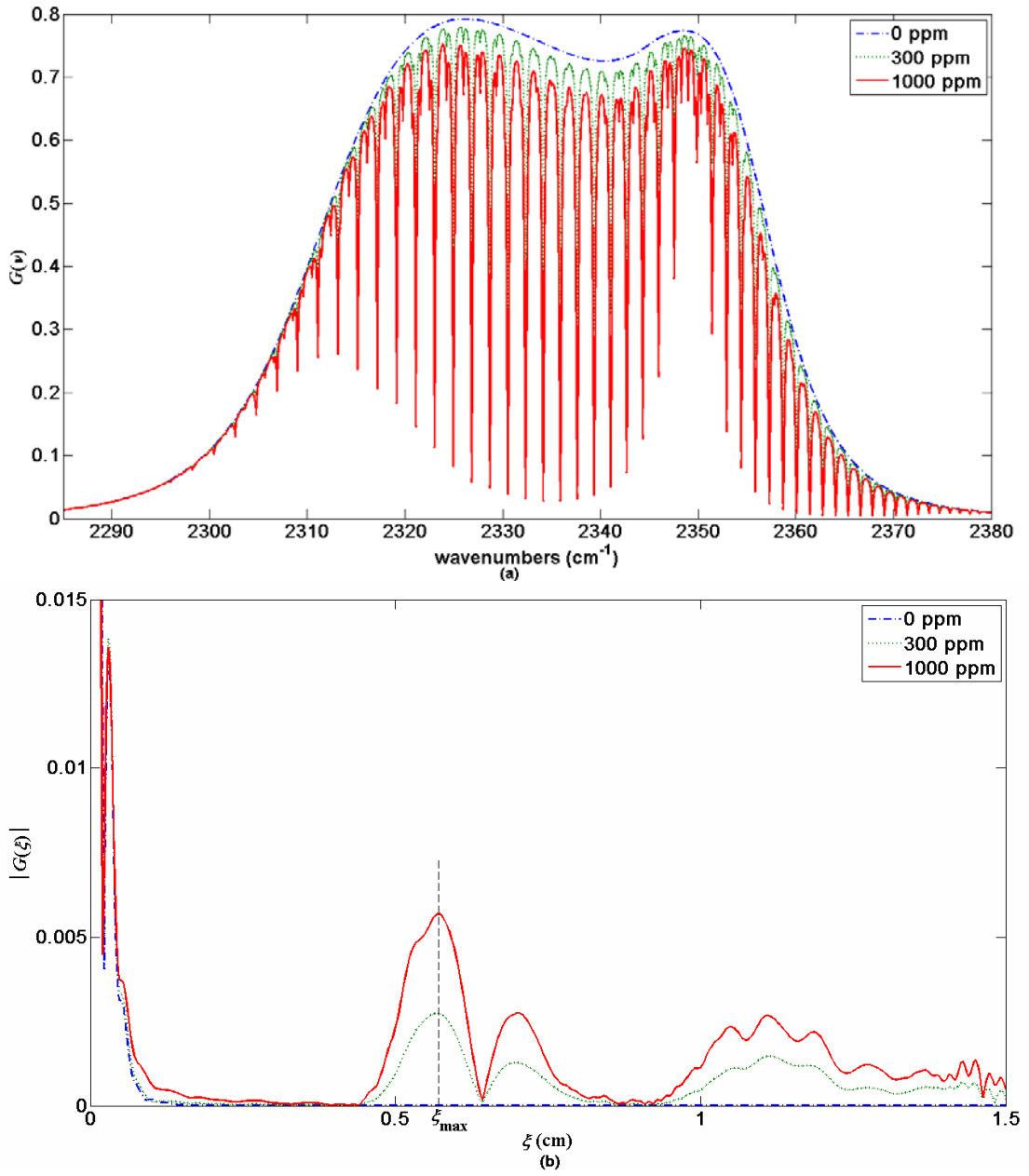


Figure 3- a) Function $G(\nu)$ profile showing the filter performance and the ro-vibrational absorption lines of $CO_2$ and considering a flat source b) Fourier transform of $G(\nu)$, here the magnitude of the side-lobes centred at $\xi = 0.56$ cm clearly increase with the $CO_2$ concentration.

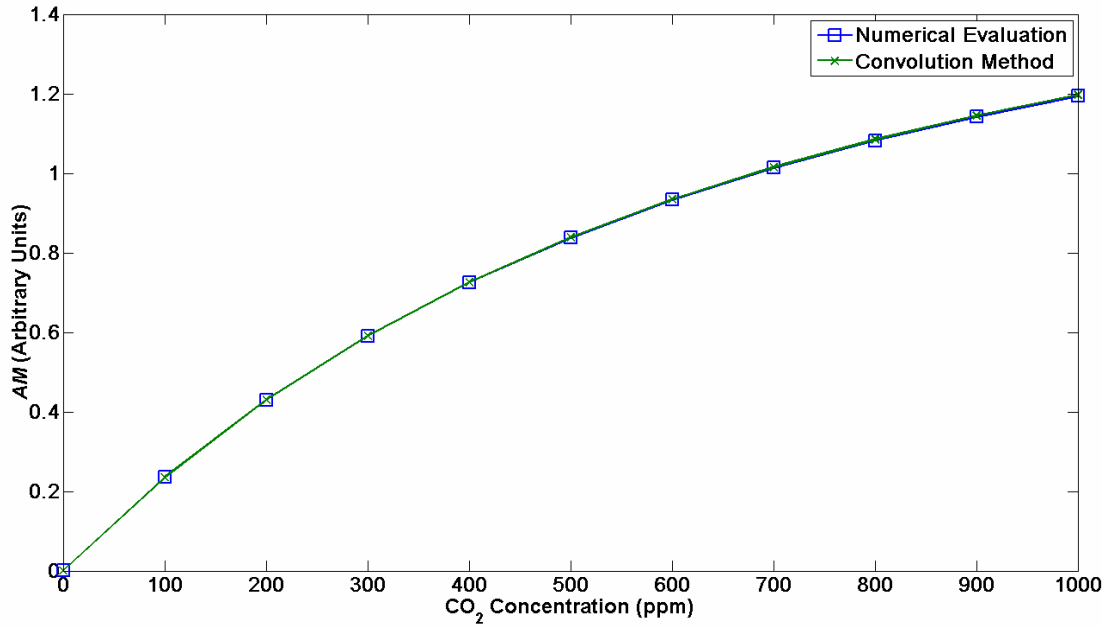


Figure 4- Amplitude Modulation for a $CO_2$ sensor evaluated using both the Direct numerical evaluation of equation (1) and using the convolution method. Here $R = 0.30$ and $nd = 0.28$ cm.

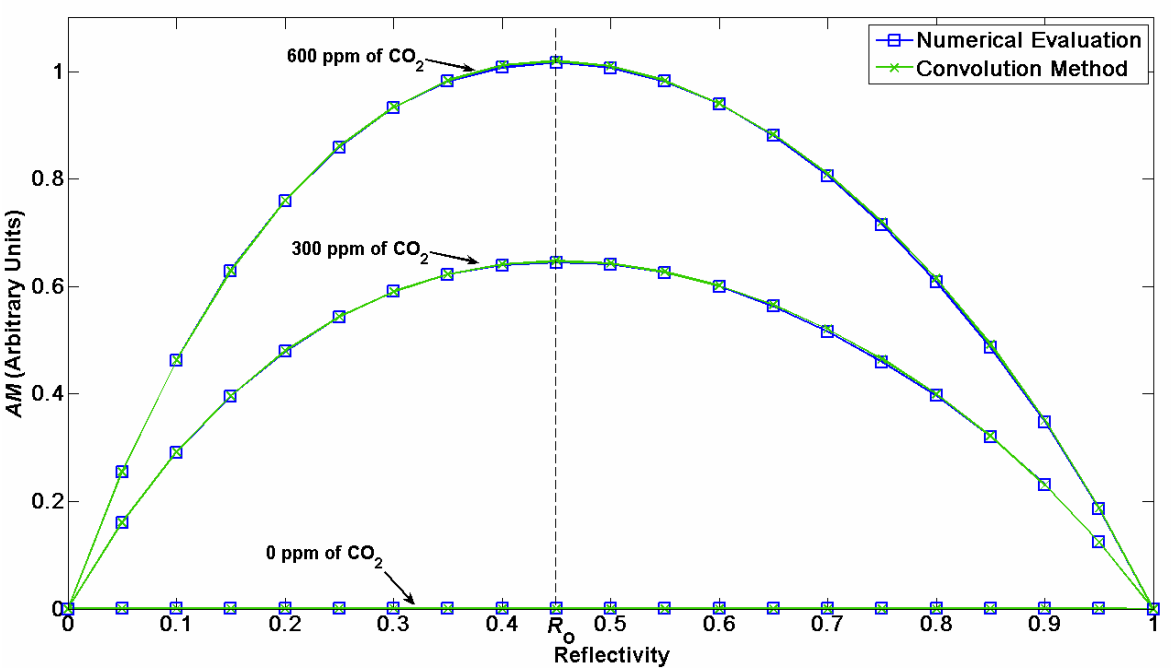


Figure 5- Amplitude modulation as a function of the reflectivity with a constant optical thickness $nd = 0.28$ cm. Different $CO_2$ concentrations are shown.

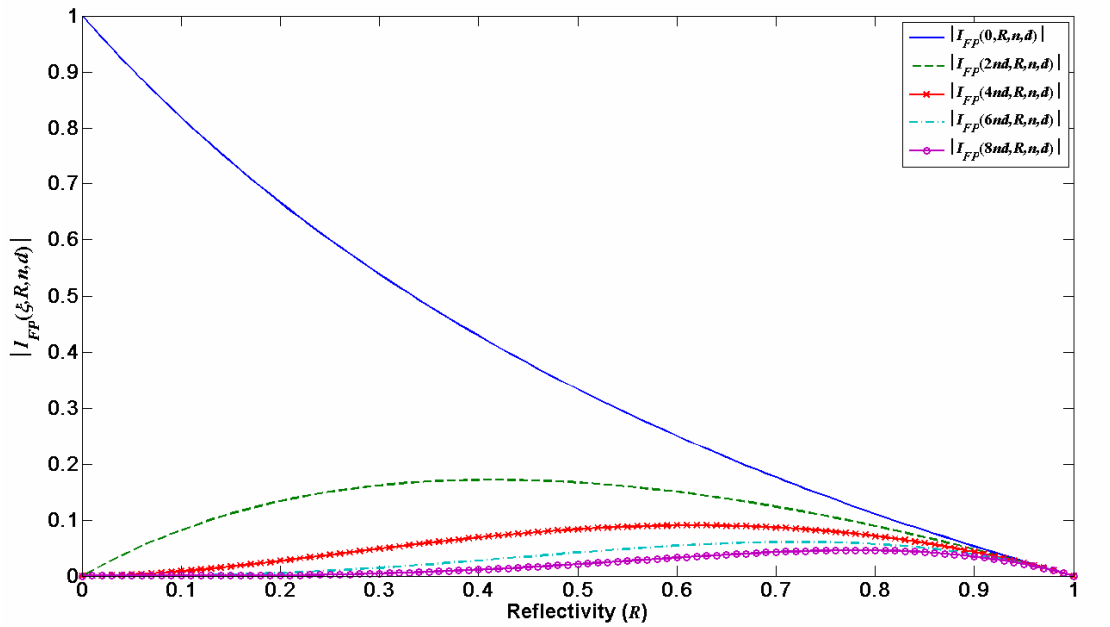

Figure 6- Magnitude of the FPI fringes impulses as a function of the reflectivity.

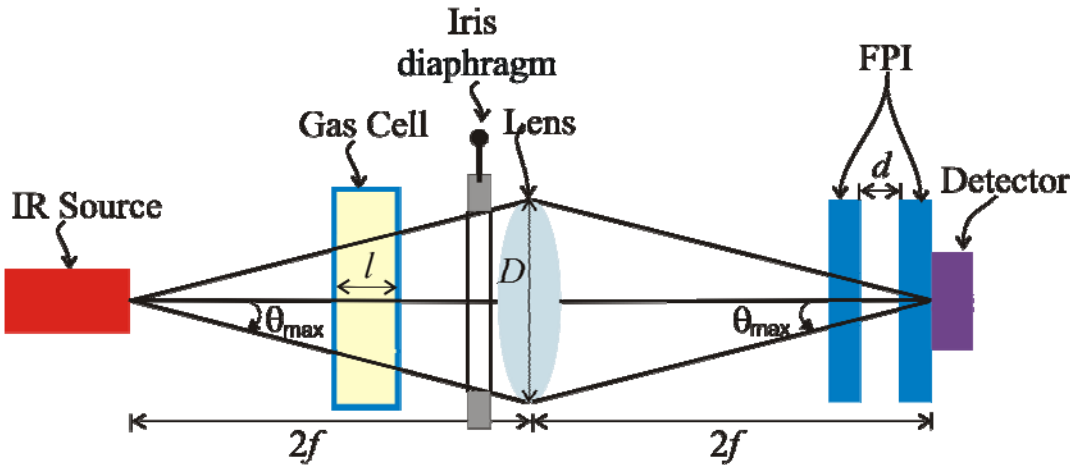

Figure 7- Experimental Setup.

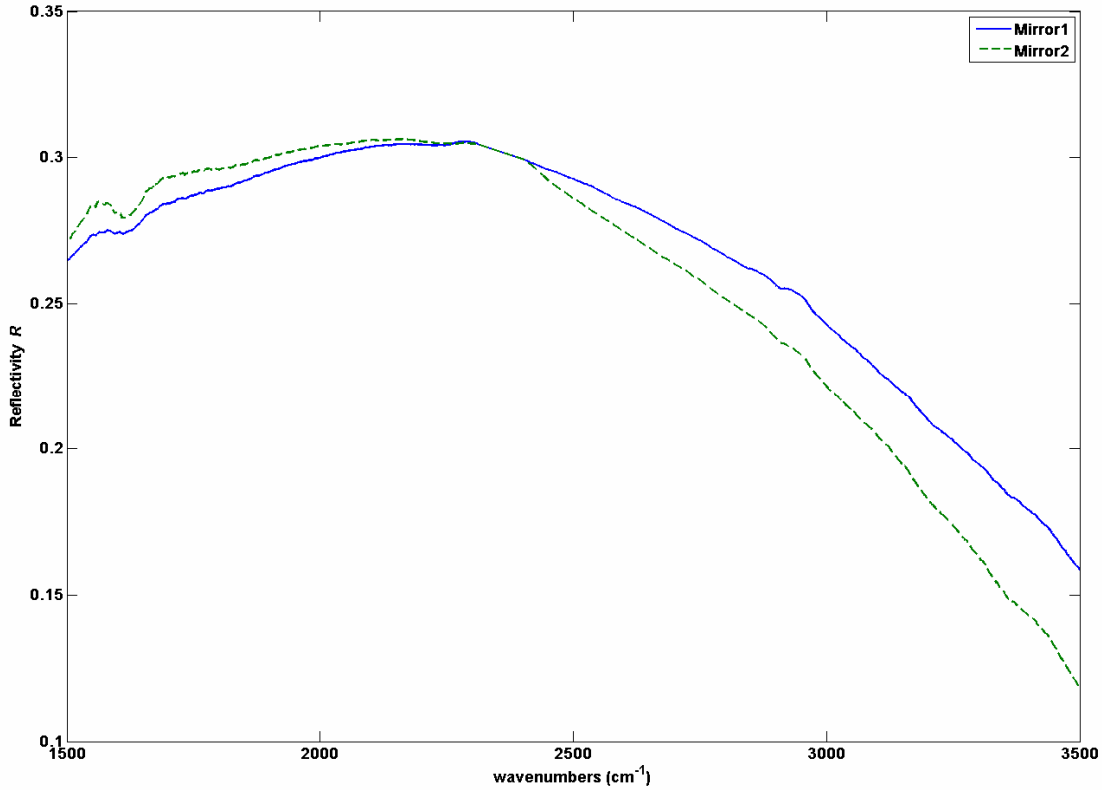

Figure 8- Measured FPI Mirror reflectivity.

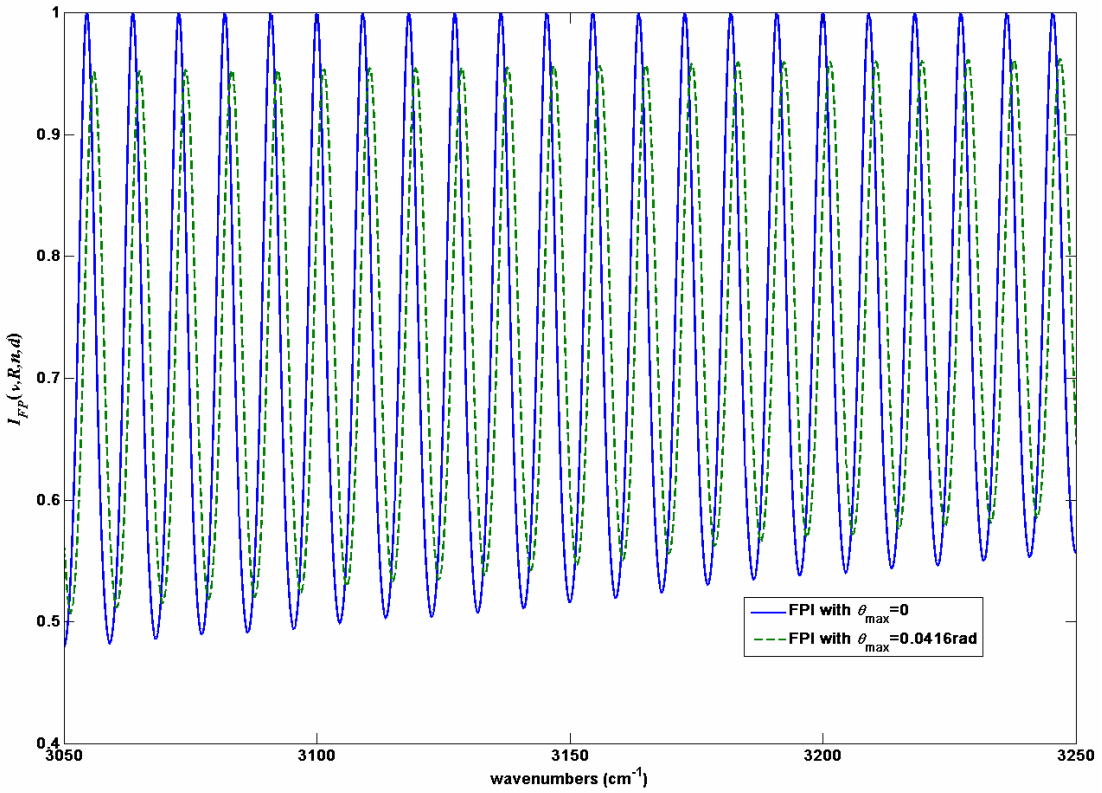


Figure 9- FPI fringe patterns evaluated for a collimated beam $(\theta_{\max} = 0\text{rad})$ and for a converging beam with $\theta_{\max} = 0.0416$ rad.

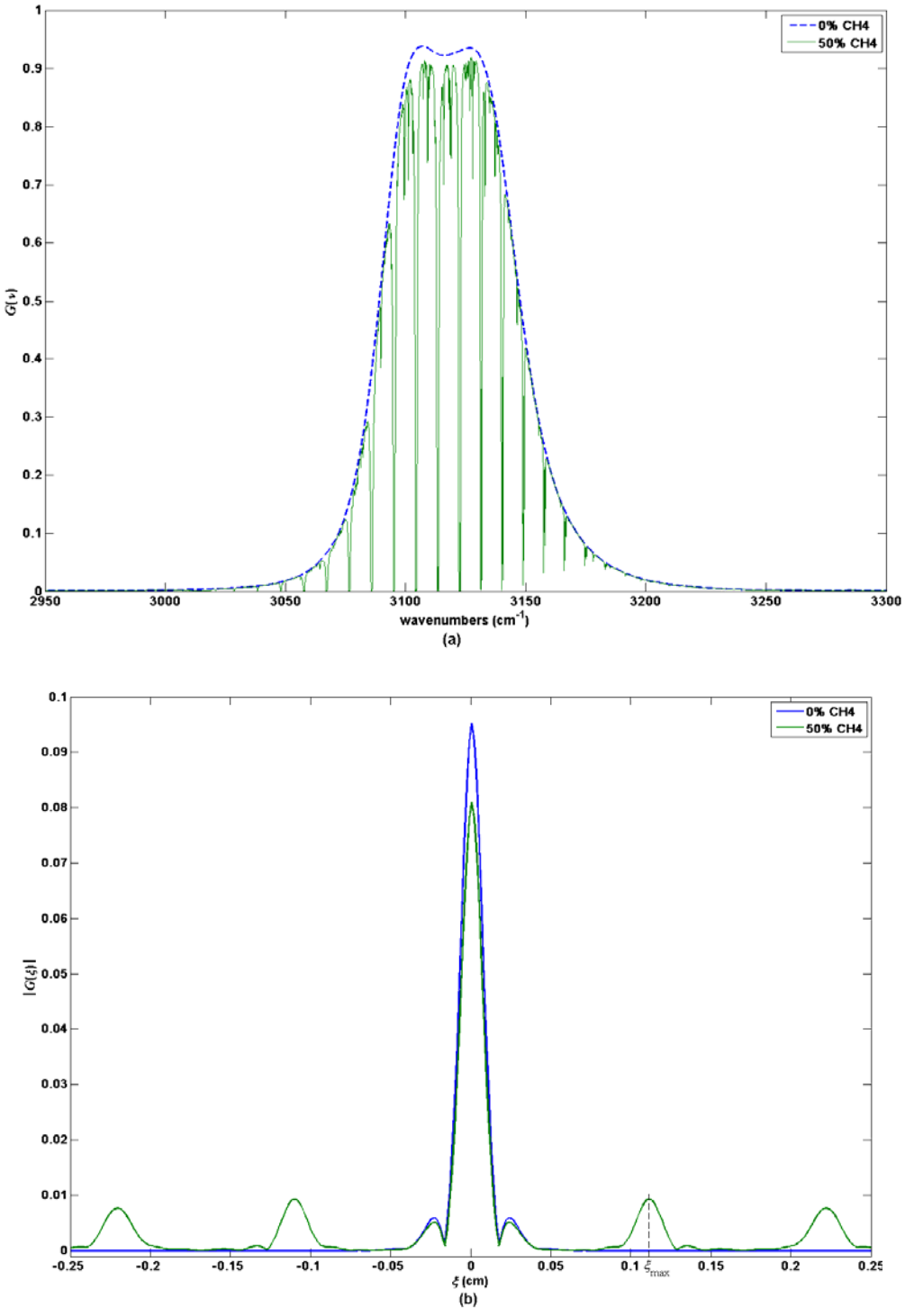


Figure 10- a) Function $G(\nu)$ for the $CH_4$ sensor for different gas concentrations. b) Magnitude of the Fourier transform $|G(\xi)|$.

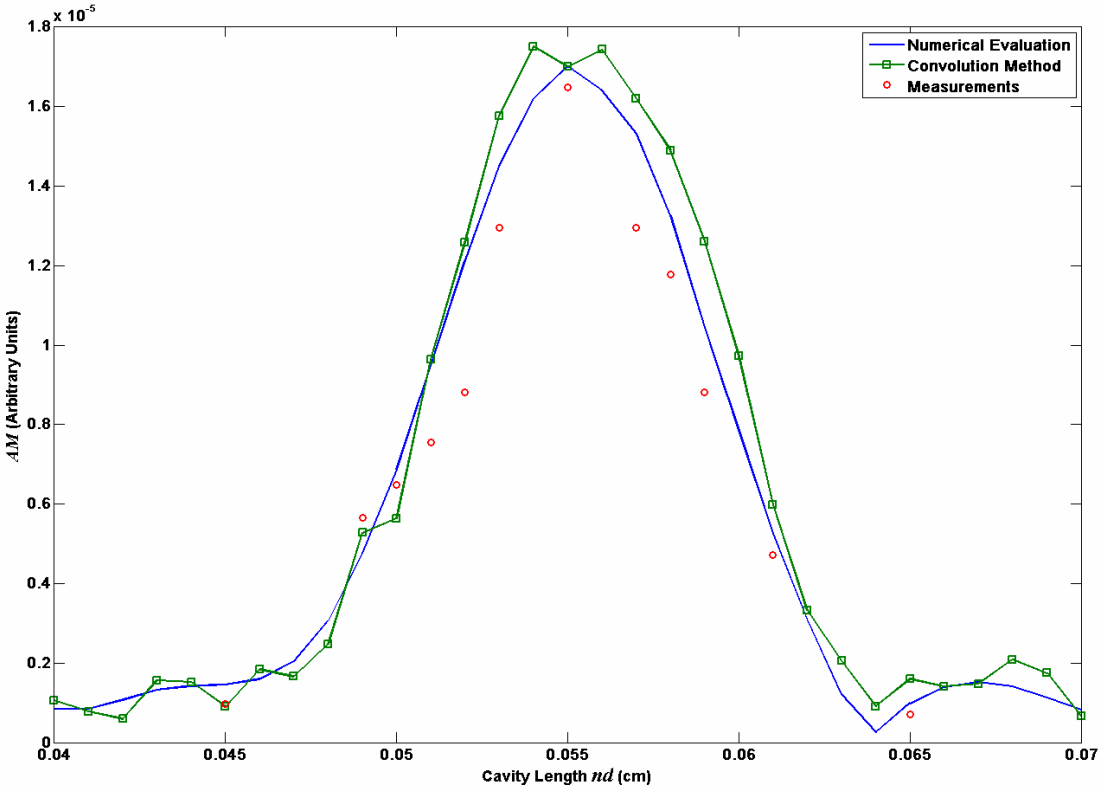


Figure 11- Simulated and Measured Amplitude Modulation values for the $CH_4$ sensor. Here we use $R = 0.30$ and $CH_4$ Concentration of 50%.

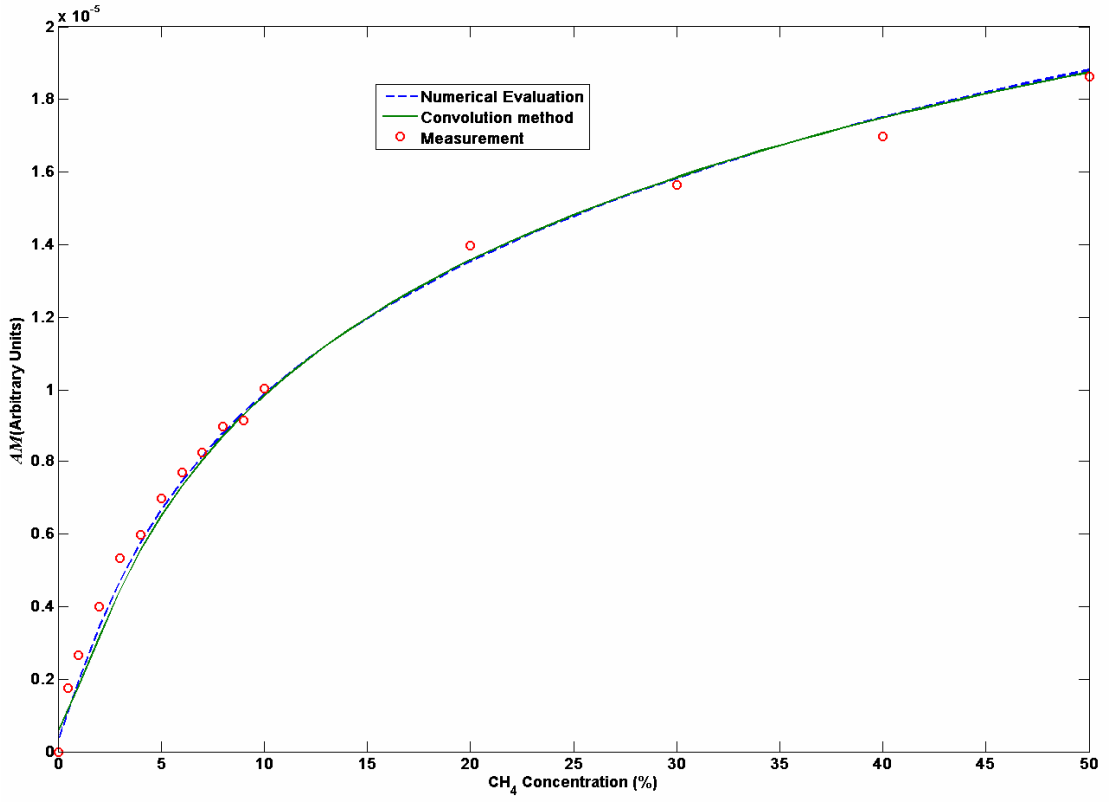


Figure 12- Simulated and Measured $AM$ values in function of the $CH_4$ Concentration.